Version v4 2005, December 14th
Orsay-ALICE Group

Summary of the geometry and segmentation parameters used for Station1 in the simulations (AliRoot)

The main objectives of this document are:
1) Listing the actual status for the station1 geometry as:
- the quadrant structure including values for material thicknesses
- The pads and wires position in the general frame of ALICE Dimuon arm.

2) Listing the checks performed using the code AliRoot to compare the values introduced in this code with the values given for mechanical structures and segmentation by the constructors.
Besides a careful study of the values set in the code, dimuon events were generated randomly. Position reconstruction of hits in space (XYZ) was checked through transport of particles, digitization of hits and clusterization. The new geometry framework was used in AliRoot code.

Conventions:
Conventions for the quadrant numbering are reported for the first chamber of Station 1 in figure 1.
The first cathode plane is a Bending Plane, the second one is a non Bending Plane for quadrants 100 and 102 whereas the non Bending plane is the first one for quadrants 101 and 103 (considering particles trajectories in the Z direction as presented in the figure).

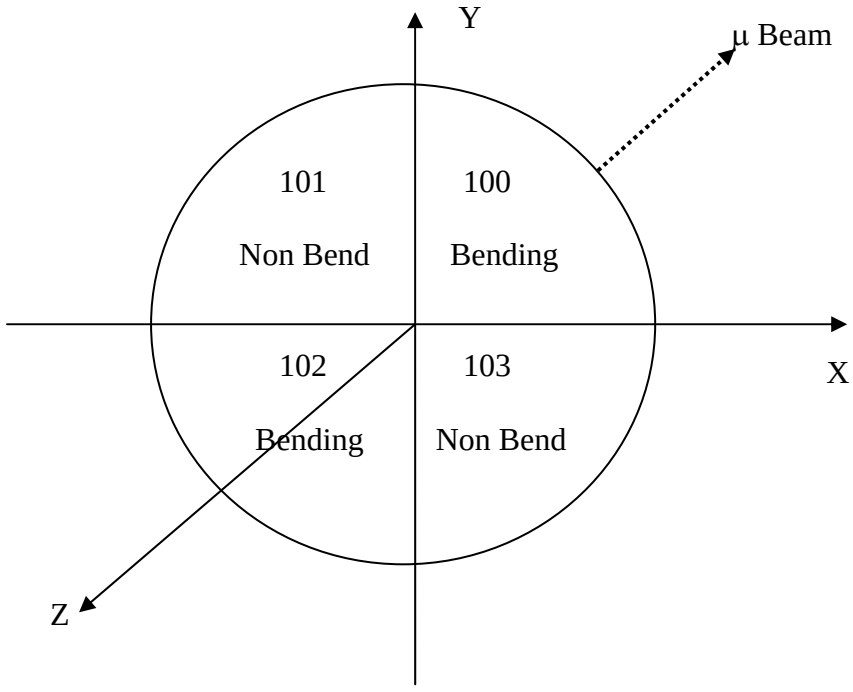

Figure 1: Conventions for quadrant numbers of chamber 1

For chamber 2, convention numbers are respectively 200, 201, 202 and 203.

Structure of one quadrant in the beam direction (OZ)

The thicknesses of the different materials are deduced from mechanical data (Ref [1]) and reported in table 1.

Component	Thick. (mm)		
MANUs	9		
PCB Electronic exit board	0.4		
Glue	0.1		
Epoxy board	0.8		
Glue	0.1		
Foam	24.2		
Glue	0.1		
Cathode PCB	0.8		
Gas	2.1		
Anode plane	0	**57.2**	**75.2**
Gas	2.1		
Cathode PCB	0.8		
Glue	0.1		
Foam	24.2		
Glue	0.1		
Epoxy board	0.8		
Glue	0.1		
PCB Electronic exit board	0.4		
MANUs	9		

Table 1: Thicknesses (mm) of the successive layers of a quadrant

It was mandatory to check (and to modify if necessary) the following data:
Anode-cathode gap (2.1 mm) is found correct.
Pad dimensions (Ref [2]) *for the 3 different zones are correct.*

Wire position with respect to pad limits:

(Used to calculate integration limits of Mathieson function for example)
Theoretical scheme is given in figure 2 for the central zone.

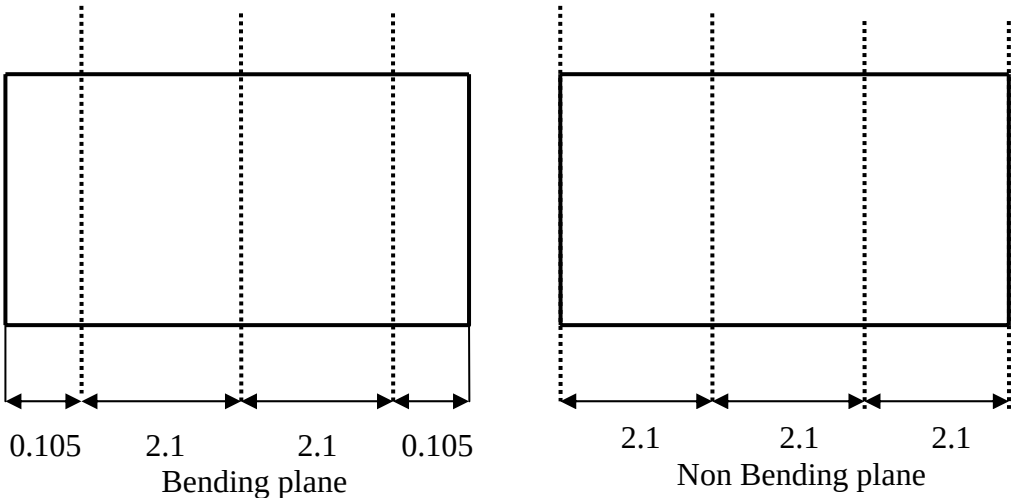

Figure 2: Wire positions/ pads for the central zone (mm)

Geant hits are first calculated and the avalanche position is set on the nearest wire (by means of (SetHit(GetAnod(…)) function before distributing the charge on the pads.

The wire position (number of the wire) is in agreement with the mapping of the pads in the bending plane as in the non bending plane. The anode pitch is used.

Anode Pitch: *was modified in the code. (2.1 mm instead of 2 mm)*

To be discussed: Charge is entirely on one wire even if the track is far from the wire.

Position of quadrants along the beam direction:

It has to be reminded that chambers are **perpendicular** to the beam axis.

Using hit positions in the Muon StepManager, z *positions are now corresponding to the foreseen mechanical positions as given in table 2 for the different quadrants.*

To be noticed:
The anode position along the beam (Z axis) direction is not included in the geometry package of the code but is calculated for each track from the position of the entrance and exit of the trajectory in the sensitive volume (DeStep and DeStepSum variables)
This point should be discussed as the avalanche is on the wire theoretically.

Distances between quadrants of a chamber and between chamber 1 and chamber 2 are in accordance with the mechanical values of table 2.

		ELEMENT	Z(CM)
		Entrance of the electronic plane	-518.45
		Entrance of the gas volume	-522.2
	Quadrants 100 and 102	**Anode plane (z first quadrant)**	**-522.41**
		Exit of the gas volume	-522.62
		Exit of the electronic plane	-526.37
Chamber 1		***z first chamber***	***-526.16***
		Entrance of the electronic plane	-525.95
		Entrance of the gas volume	-529.7
	Quadrants 101 and 103	**Anode plane (z second quadrant)**	**-529.91**
		Exit of the gas volume	-530.12
		Exit of the electronic plane	-533.87
		z station 1	***-535.7***
		Entrance of the electronic plane	-537.53
		Entrance of the gas volume	-541.28
	Quadrants 200 and 202	**Anode plane (z third quadrant)**	**-541.49**
		Exit of the gas volume	-541.7
		Exit of the electronic plane	-545.45
Chamber 2		***z second chamber***	***-545.24***
		Entrance of the electronic plane	-545.03
		Entrance of the gas volume	-548.78
	Quadrants 201 and 203	**Anode plane (z fourth quadrant)**	**-548.99**
		Exit of the gas volume	-549.2
		Exit of the electronic plane	-552.95

Table 2: Position of elements in the chambers along the beam axis (cm)

Lateral position (X and Y) of the quadrants with respect to the beam.

Comparison between the hit position from the tracking and the mapping calculations with local to global frame transformations is checked.
The shifts between the relative position of the pads for the bending and non bending plane were checked (a shift by half a pad in X and Y direction was foreseen). The calculated values are now in accordance with the theoretical mechanical values quoted in tables 3 and 4.

Quadrant Number	Distance from the beam axis to the centre of the first pad column(X) or row(Y)			
	BENDING		NON BENDING	
	X (cm)	Y (cm)	X (cm)	Y (cm)
100	-0.3100	0.5000	-0.1000	0.1850
101	-0.3100	-0.5000	-0.1000	-0.1850
102	0.3100	-0.5000	0.1000	-0.1850
103	0.3100	0.5000	0.1000	0.1850

Table 3: Distances (cm) between the middle of the first column or row of pads and the beam axis

Quadrant Number	Distance from the beam axis to the external border of the first pad line or row			
	BENDING		NON BENDING	
	X (cm)	Y (cm)	X (cm)	Y (cm)
100	-0.5200	0.1850	-0.3100	-0.1300
101	-0.5200	-0.1850	-0.3100	0.1300
102	0.5200	-0.1850	0.3100	0.1300
103	0.5200	0.1850	0.3100	-0.1300

Table 4: Distances (cm) between the external border of the first column or row of pads and the beam axis

These values are quoted in figures 3 to 6.

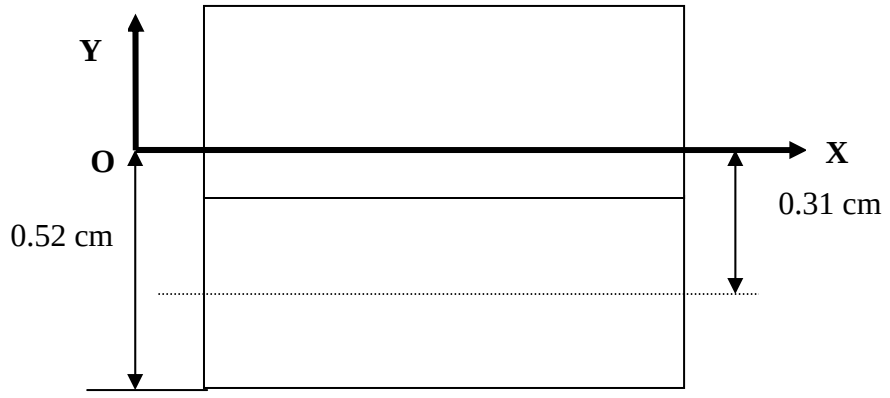

Figure 3: Bending plane for quadrant 100

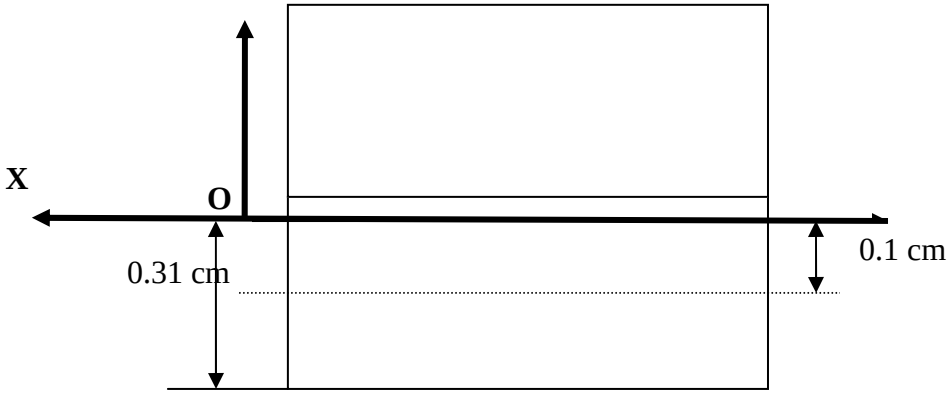

Figure 4: Non Bending plane for quadrant 100

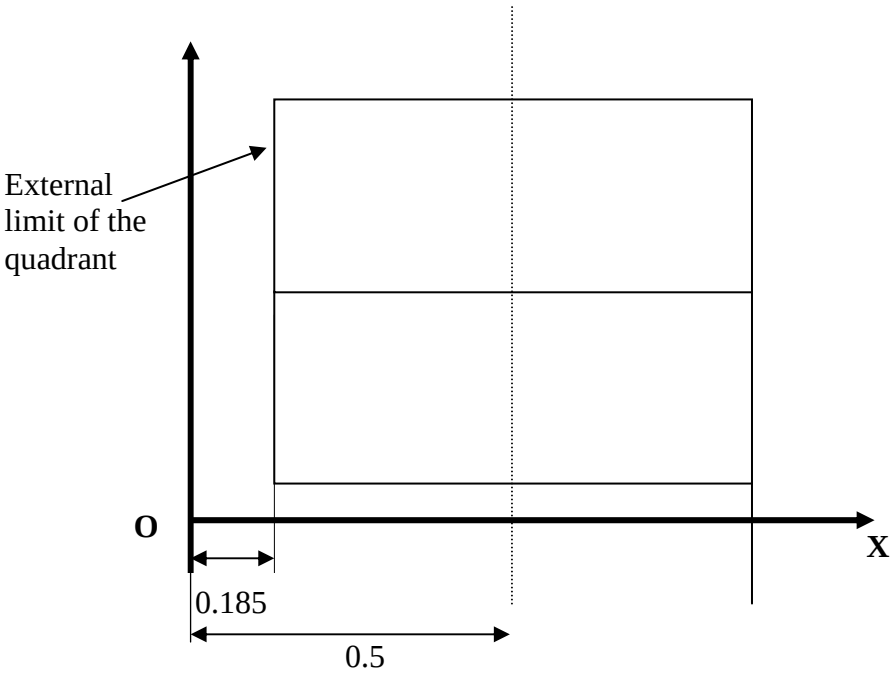

Figure 5: Bending plane of quadrant 100 (distances in cm)

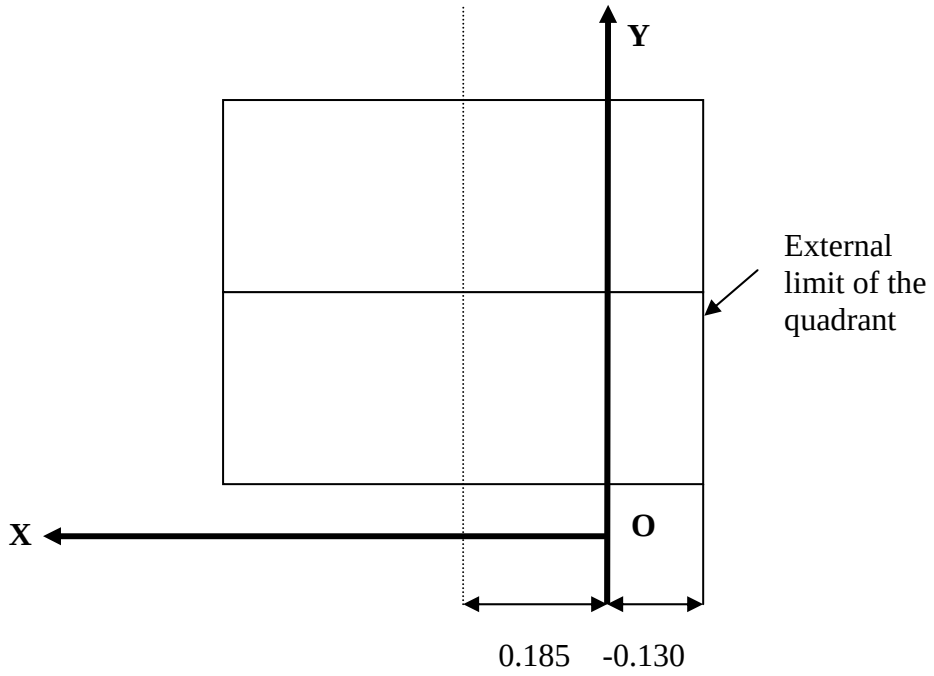

Figure 6: Non Bending plane of quadrant 100 (distances are given in cm)

Structure of the chamber:

The different parameters (thickness and shape of the materials) were those of the previous first prototype.

These parameters have to be changed in concordance with the last version of the detector.
Mainly, the foam thickness is now 2.503 cm instead of 2.083 cm (4.2 mm more than the old geometry) and the FR4 thickness is changed from 0.4 mm to 0.8 mm. Equivalent value introduced in Ref [3] to take into account the inhomogeneities is changed from 0.031 cm to 0.062 cm.
A study of the effect of these changes has been performed specially for FR4. Results are summarized in table 6 for 0.0031, 0.031 cm and 0.062 cm FR4 thickness . For this purpose, 5000 J/Psi were generated without background. Changes were only done for FR4 in station1.
A second set of 5000 J/psi has been generated in order to see statistical effects.
Several remarks can be extracted from table 6:

- Comparing results for the 2 different sets of J/Psi and with the same geometry (column 2 of table 6):
- Due to multiple scattering and physics processes in materials, trajectories are different in the 2 cases. So statistical effects are important. Fluctuations of 1.3% are observed in the J/Psi mass region for 5000 J/Psi different sets.
- This allowed further conclusions at the level of 1% precision (hhe acceptance varies depending on the hit positions).
- Few muons are lost (see number of events with one muon hit instead of 2 in chamber1 of station1) . Corresponding events have generally no electrons hits.

- *Reconstruction inefficiency (clustering) is around 2.6% which seems to be not very good for very "clean events" without background. Percentage of events with contamination of electrons is around 3.3%.*
- Introducing different thicknesses for FR4 (columns 2-3-4) for the same set of 5000 J/Psi:
- The effect of introducing 310 microns instead of 31 microns FR4 (twice per chamber of station one) is around 0.5 % loss on the number of reconstructed J/Psi in the mass spectrum. The effect is of the same order for a 620 microns FR4 thickness, i.e in the 1% precision range.
- It can also be noticed that the radiation length for FR4 is taken as 19.4 cm (ref. 3) which is a large value compared to (0.031 cm *4) 0.124 cm thickness value introduced in the code.

-It will be worthwhile to introduce a realistic structure of the detectors to get 1% precision level on the efficiencies.

	1	2	3	4
Structure St1 Thickness		FR4 0.0031 cm	FR4 0.031 cm	FR4 0.062 cm
5000 Jpsi are generated	Events in Mass range (1.5-4 GeV/c^2)	3239	3218	3235
	Event in mass range (2.8-3.8 GeV/c^2) +chi2+ptcut	3205	3189	3196
	Events with 1 muon in ch1 st1 instead of 2 (hits)	24	22	32
	1 recpoint only in ch1 st1 (after cluster)	129 excluding previous 24	135 excluding previous 22	119 excluding previous 32
	Nb events containing with electrons	185	163	179
Another set of 5000 Jpsi (different seed)	Mass range (1.5-4 GeV/c^2)	3277		
	Event in mass (2.8-3.8) +chi2+pt cut	3247		
	1 muon in ch1 st1 instead of 2 (hit)	15		
	1 recpoint only (after cluster)	155 containing 15		
	Nb events with electrons	165		

Table 6 :Number of events in each specified case

Various items:

- Concerning the geometry for station1: the central point is not introduced in the simulation. Frames outside the sensitive zone have not been updated.
- Concerning the inclined tracks: Parameterization from K. Boudjemline Ref.[4] is currently used to take into account angles lower than 9.2^0

- Concerning the clusterization algorithm: ClusterFinderVS module was used.

Some inconsistencies were found for one “standard“ hit for which 2 clusters were found. In this case it was observed also that the reconstructed point was not on a wire position.
To be re-discussed: use of clusterFinderVS or AZ modules in the code?

- Concerning pedestal subtraction and threshold:

Files for electronic pedestals and noises are ready and should be filled with values from measurements for each electronic channel.

Three options are ready and are tested (D. Guez and M Mac Cormick) (Ref [5]):

- Without pedestals and noise.
- Pedestals and noises randomly distributed following one gaussian law for each channel.
- Pedestals and noises read from a file.

Architecture of this part has to be reconsidered in order to be used for real data.
This work is now undertaken by A. Charpy and I. Hrivnacova

References

1] J. Peyré et al. Orsay ALICE-INT-1998-28 “A Full-scale prototype for the tracking chambers of the ALICE muon spectrometer Part I- Mechanics; Anode and Cathode palne design; Assembly and Construction”.

2] ALICE-INT-2003-035 v.3 “Results of the In-Beam tests performed with the Quadrant 0 of Station 1 for the ALICE Dimuon Arm”.

Dimuon forward Spectrometer. Addendum 1 to ALICE TDR 5-CERN/LHCC 2000-046.

3] ALICE Orsay group – Internal note IPNO-DR-02-010 « Matériaux, X_0 et sections géométriques du quadrant zéro du spectromètre dimuons d’ALICE ».

4] Thesis : K. Boudjemline (Nantes 2004).

5] Thesis : D. Guez, IPNO-T-03-05, (Orsay 2003).